

light yellow and then pale green with fluorescence. After 1 hr, an olive green powdery solid began to separate. The mixture was left overnight at room temperature. The solid was filtered on a Büchner funnel, washed with ice-cold  $\text{CCl}_4$ , and dried *in vacuo* over  $\text{P}_2\text{O}_5$ . Osmium was determined by our slight modification of Criegee's method.<sup>1</sup> The oxidation state of osmium in the esters and other compounds was determined by iodometric analyses as follows (Table I): 15–85 mg of the compound was dissolved in water. Ten milliliters of 0.4 *N* KI was added followed by 5 ml of 2 *N* sulfuric acid and 25 ml of chloroform. The pyridine and picoline esters gave a violet-brown chloroform layer and a dark green aqueous layer. The mixtures were titrated with 0.1 *N* thiosulfate to a light olive green end point in the chloroform layer. Carbon, hydrogen, and nitrogen analyses were performed by Galbraith Laboratories, Knoxville, Tenn.

**Determination of Osmium Tetraoxide Formed Following the Hydrolysis of the Esters.**—A spectrophotometric or a titrimetric method was used depending on the amount of ester. Ester (2–60 mg) was added to water or to dilute sulfuric acid in 25-ml standard flasks. Acid solutions rapidly gave a clear supernatant fluid and a black precipitate. Anhydrous sodium sulfate was added to coagulate the solid. The mixture was filtered through a sintered glass funnel using as little suction as possible ( $\text{OsO}_4$  is volatile). The absorbancy ratio, 240/300, can be used to demonstrate the absence of Os(VI) species from these solutions. For  $\text{OsO}_4$ , the ratio is 2.0 and  $\epsilon_{240}$   $3150 \pm 50$ . The Os(VI) species all have maxima in the vicinity of 300 nm; *e.g.*, potassium osmate has  $\epsilon_{300}$   $1200 \pm 100$ . The titrimetric method was used for larger quantities. In this case, the filtrate was collected directly into a mixture of 10 ml of 0.4 *M* KI, 5 ml of 2 *N*  $\text{H}_2\text{SO}_4$ , and 25 ml of chloroform. A violet chloroform layer and a dark green aqueous layer were formed. The mixture was titrated to a colorless end point in the chloroform layer using 0.1 *N* thiosulfate.

**Analysis of the Black, Insoluble Osmium Oxides.** (a) **The Initial Precipitate.**—Thirty to fifty milligrams of the CCA ester was added to 150–200 ml of water and allowed to stand at room temperature for 30–45 min to ensure complete hydrolysis. A blue-black colloidal suspension formed within a few minutes. After 30–45 min to ensure complete hydrolysis, solid sodium sul-

fate was added to flocculate the suspension. A clear, colorless supernatant liquid remained. If hydrolysis was incomplete, the supernatant liquid was brownish yellow. The mixture was filtered on a tared sintered-glass funnel and washed several times with water. The washings were discarded. The oxide on the filter was stirred with a 20% KI solution acidified with sulfuric acid. The filtrate was collected and the process repeated until liberation of  $\text{I}_2$  ceased.  $\text{I}_2$  in the combined filtrates was titrated with thiosulfate. The remaining precipitate was washed thoroughly with water and ether, dried *in vacuo* over  $\text{P}_2\text{O}_5$  and weighed. Similar experiments were carried out with potassium osmate except that the initial solution must be acidified because of the alkalinity of potassium osmate solutions.

(b) **The Final precipitate.**—The black precipitate initially formed is allowed to stand in a glass-stoppered flask (total volume 10–15 ml) for 10–15 days together with the osmium tetraoxide initially formed. The precipitate was washed, dried, and weighed.

**Warburg Experiments.**—CCA ester (4–5 mg) was weighed into a small glass boat which was designed to balance on top of the center well of a single-arm Warburg flask. The main compartment of the flask contained 2.5 ml of water or buffer. In some experiments, oxygen-trapping solutions were placed in the side arms. In these cases, the air in the flask was replaced with nitrogen. The ground-glass joints were sealed with syrupy phosphoric acid at the lower edge and lanolin at the upper edge. After thermal equilibration, the boat and its contents were tipped into the main compartment. Readings were taken at 30 min intervals for about 12 hr.

**Acknowledgments.**—This work was supported by the National Science Foundation, GB-21267. We thank Mr. John Ragazzo for his careful measurements of the ir spectra, Dr. George Serif for his expert help with the mass spectrometer, and Drs. Daryle Busch and J. Dabrowiak for determining the magnetic susceptibilities.

CONTRIBUTION FROM THE SCHOOL OF MOLECULAR SCIENCES,  
UNIVERSITY OF SUSSEX, BRIGHTON BN1 9QJ, ENGLAND

## The Magnetic Circular Dichroism and Absorption Spectra of Nickel(II) Oxide

By P. BRINT, A. J. McCAFFERY,\* R. GALE, AND M. D. ROWE

Received January 24, 1972

The absorption and MCD spectra of a thin film of NiO have been measured at  $\sim 8^\circ\text{K}$  and the results interpreted in terms of an exchange field splitting of the spin-orbit states using molecular field theory. The results agree well with calculation and assignments have been made. It is noted that a single ion approach is inadequate to explain both the absorption and the MCD spectra in contradiction to previous work on thin film and single crystal NiO.

### Introduction

Most studies of the electronic spectra and structure of octahedral Ni(II) complexes have been directed toward obtaining crystal-field theory information:  $\Delta$ , covalency parameters, electron repulsion parameters, low symmetry or lattice distortions, etc.<sup>1</sup> Inorganic chemists have generally tended to ignore the spectra of the binary compounds and instead have examined crystals whose spectra are similar in the solid state and in solution. In the binary oxides, for example, strong cooperative effects are a special feature of the physical properties of the compounds and in this work we have examined a crystal of markedly antiferromagnetic Ni(II) in order to characterize

the electronic states in the presence of a strong exchange field.

Nickel oxide is a particularly interesting and important compound. By contrast to the early iron group oxides it does not exhibit metallic type conduction having a conductivity of  $10^{-8} \text{ ohm}^{-1} \text{ cm}^{-1}$ .<sup>2</sup> This fact necessitated some rethinking of the approach to the theory of electrons in solids since according to the band theory, NiO should have a partly filled d band and thus be an excellent conductor. However, it is not and, furthermore, the electronic spectrum is similar to that of  $\text{NiSO}_4 \cdot 7\text{H}_2\text{O}$ , say, or to Ni(II) in aqueous solution. Thus a Heitler-London or localized electron model of the electronic structure of NiO is more

(1) See for example J. Ferguson, *Progr. Inorg. Chem.*, **12**, 159 (1970).

(2) J. P. Suchet, "Crystal Chemistry and Semiconduction," Academic Press, New York, N. Y., 1971, p 169.

appropriate than the "delocalized" band theory approach and the justification for this was given some years ago by Mott.<sup>3</sup> He showed that as the nuclear separation of a delocalized system is increased, a sharp transition to the localized state occurs with consequent drop in conductivity. In NiO the interionic distances are sufficient to prevent the degree of overlap needed for metallic conduction and the electrons are bound strongly to a particular metal ion.

Despite the absence of metallic conduction, conditions for magnetic interactions between the ions are fulfilled and NiO is strongly antiferromagnetic with  $T_N = 523^\circ\text{K}$ .<sup>4</sup> Neutron diffraction studies show<sup>5</sup> that exchange interaction occurs *via* the  $e_g$  electrons on next nearest neighbors *via* intervening oxide ions. This mechanism, known as superexchange, is a maximum when the M-O-M angle is  $180^\circ$ . In NiO the exchange interactions are particularly strong. In any description of the electronic states of NiO, therefore, the effect of the exchange field must be taken into account.

Although it is known that strong exchange forces exist in NiO, previous studies of its electronic spectrum are characterized by the neglect of this effect.<sup>6,7</sup> In a study of single-crystal NiO and of oxidized films of nickel metal, Newman and Chrenko<sup>6</sup> concluded that the tight binding approximation was adequate for the infrared and visible absorption bands and that the spectra were those of simple crystal field perturbed Ni(II) ion. A similar conclusion is implicit in the more recent work of Ueno and Mayashi.<sup>7</sup> This assumption is unreasonable for a precise description of the electronic states since the exchange field is at least comparable to spin-orbit coupling and therefore, at low temperatures, splittings should be seen. Furthermore, the exchange field should remove the degeneracy of the single-ion ground state completely, leaving only the sublattice degeneracy. This will affect the selection rules for the absorption of light. The spectra of NiO should therefore show significant differences from those of  $\text{Ni}^{2+}$  doped into MgO or  $\text{NiSO}_4 \cdot 7\text{H}_2\text{O}$  and the new features which might be expected to emerge are (a) a different number of bands, (b) shifts of bands, and (c) enhancement of the intensity of the spin forbidden bands.

The absorption spectrum of NiO shows certain similarities to that of  $\text{MgO}:\text{Ni}^{2+}$ <sup>8</sup> as expected since the major interactions are the crystal field and electron repulsions. The MCD spectrum shows very marked differences to the nonmagnetically coupled Ni(II)-containing crystals at low temperatures and on closer examination, there are distinct differences in the absorption.

### Experimental Section

The sample used for this work consisted of a film of NiO coated on a crystal of MgO, and it was obtained from the Clarendon Crystal Growing Laboratory, Oxford, through Dr. S. J. Smith. It was mounted in the bore of a superconducting magnet and its spectra were measured at  $\sim 8^\circ\text{K}$  and at room temperature. The

(3) N. F. Mott, *Phil. Mag.*, **6**, 287 (1961).

(4) J. B. Goodenough, "Magnetism and the Chemical Bond," Interscience, New York, N. Y., 1966, p 88.

(5) (a) C. G. Shull, W. Strauser, and E. O. Wollan, *Phys. Rev.*, **85**, 333 (1951); (b) W. Roth, *ibid.*, **110**, 1333 (1958).

(6) R. Newman and R. Chrenko, *ibid.*, **144**, 1507 (1959).

(7) T. Ueno and M. Mayashi, *J. Phys. Soc. Jap.*, **22**, 1305 (1967).

(8) (a) W. Low, *Phys. Rev.*, **109**, 247 (1958); (b) R. Pappalardo, D. L. Wood, and R. C. Linares, *J. Chem. Phys.*, **35**, 1460 (1961).

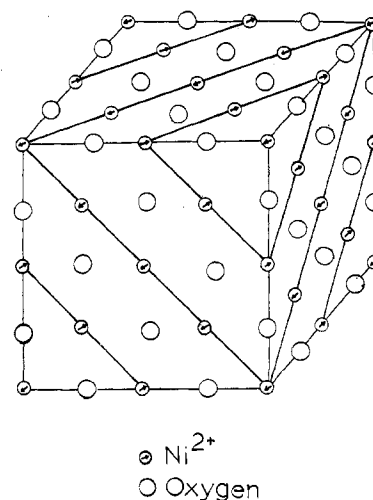


Figure 1.—The magnetic structure of NiO showing the spins  $M_s = +1$ ,  $M_s = -1$  in alternate (111) planes.

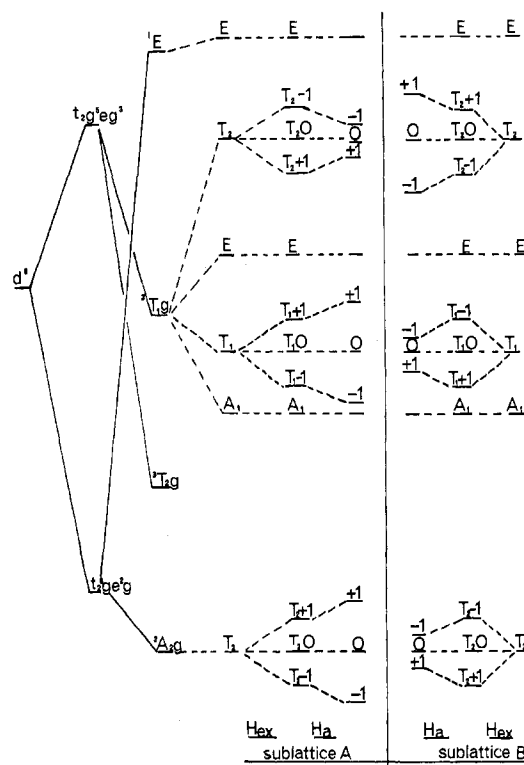


Figure 2.—The energy levels of the ground state and "red" band region of  $\text{Ni}^{2+}$  perturbed successively by (a) crystal field, (b) spin-orbit coupling, (c) exchange field, and (d) external field.

MCD was measured on a CD spectrometer originally built at the National Physical Laboratory and modified by the authors. The absorption spectrum was obtained on a Cary 14.

### Theory

The structure of nickel oxide is shown in Figure 1. It is a face-centered cubic lattice in which the nickel atoms occupy octahedral sites. At low temperatures a very slight rhombohedral distortion is known to occur, and we have assumed this effect to be small compared to spin-orbit and exchange forces.

The crystal-field states of octahedral  $\text{Ni}^{2+}$  are well known and are shown in Figure 2. Spin-orbit coupling splits these states, giving the energy level pattern shown

in Figure 2 where the octahedral double group ( $O^*$ ) functions have been obtained using the coupling tables of Griffith,<sup>9</sup> and the splittings were calculated using the irreducible tensor method.<sup>10</sup> Note that in this, as in any even-electron problem, no new irreducible representations are required to span the double group and hence we may use the familiar representations A, E, T, etc. This is felt to be a better form of nomenclature than the  $\Gamma_1$ - $\Gamma_8$  used by Ballhausen and Liehr, for example,<sup>11</sup> since the absence of the spin superscript tells us that the representations are coupled functions.

The spin-orbit constant  $\xi$  for  $Ni^{2+}$  is  $650 \text{ cm}^{-1}$ ,<sup>12</sup> and we have used this figure in the calculation. Splittings due to the exchange field must now be calculated. Since these are of similar magnitude to the spin-orbit splitting we should strictly carry out a complete diagonalization in both these perturbations. However, to simplify the calculations we have assumed as a zero order approximation that the spin-orbit states are a basis for the exchange field perturbation. We find experimentally that this procedure accounts well for the observed splittings. The crystallographic unit cell of NiO is shown in Figure 1. Neutron diffraction work shows the magnetic unit cell to be just twice the crystallographic cell.<sup>13</sup> The structure therefore consists of two interpenetrating sublattices with opposite spins on each. Ions having a particular spin form alternate (111) planes and thus the magnetic structure is alternate sheets of nickel atoms with opposite spins linked by the oxygen atoms. At low temperature a spontaneous magnetization takes place with ions on sublattice A having spins parallel to a  $C_3$  axis and those on sublattice B being antiparallel to this axis. The exchange interaction can be quantized using molecular field theory.<sup>14</sup> This is a phenomenological approach in which the effect of the surrounding ions of opposite spin on a particular  $Ni^{2+}$  ion is represented by an effective magnetic field, the magnitude of which is determined by experiment (usually from susceptibility measurements). Its effect is to remove all spin degeneracies leaving  $M_s$  or  $M_J$  as a good quantum number. Thus the spins referred to in the foregoing discussion are  $z$  components of spin, not total spin quantum numbers. For the  $Ni^{2+}$  ion having a single ion  ${}^3A_2$  or  $T_2$  ground state, the exchange field splits the  $S = 1$  degeneracy into its  $+1, 0, -1$  components. On sublattice A the  $M_s = -1$  state is lowest; on B,  $+1$  is lowest in energy. The exchange field interaction can be represented by the operator  $\pm 2\beta \cdot H_E S_Z$  where  $2\beta H_E = kT_N$  ( $375 \text{ cm}^{-1}$ ) and the sign is determined by which sublattice the ion belongs to. Initially we use the ground-state effective field operator to calculate splittings though this may be modified in the excited state.

The effect of this operator on the spin-orbit states of NiO is shown in Figure 2, and we have shown the states of sublattice A and sublattice B together with the effect of the applied magnetic field (in the MCD experiment) on each. In discussing the absorption

spectrum we need only consider one of the sublattices, since unpolarized radiation is incapable of distinguishing the sign of the  $M_s$  components. Circularly polarized light is, however, capable of distinguishing the sign since this radiation has well-defined angular momentum and we need to consider both sublattices in the discussion of the MCD spectrum.

The MCD and absorption spectra are shown in Figures 3 and 4 at  $\sim 8^\circ \text{K}$ . We focus first on the bands in the red region of the spectrum, namely, the  ${}^3T_1$ ,  ${}^1E_g$  levels. The ground-state-exchange field splitting is  $375 \text{ cm}^{-1}$ , and thus at low temperature we need only consider the lowest level on each sublattice,  $T_{2-1}$  on A and  $T_{2+1}$  on B.

Looking first at sublattice A, we first calculate the selection rules for absorption of unpolarized radiation and show that six distinct transitions are expected in this region. First note that transitions to  ${}^3T_{1g}$  and  ${}^1E_g$  are forbidden by two or more mechanisms. Those to  ${}^3T_{1g}$  are forbidden by parity and by symmetry ( $T_1 \times A_2$  does not contain the symmetry of the operator); transitions to  ${}^1E$  are spin-forbidden also. Assuming the parity rule to be overcome by the usual mechanism we may obtain symmetry allowedness by permitting mixing through the spin-orbit operator of states from  ${}^3T_2$  with excited-state  ${}^3T_1$  and with ground-state  ${}^3A_2$ . We may calculate the extent of this as is illustrated for the mixing of  ${}^3T_2$  with excited-state  ${}^3T_1$

$$|{}^3T_1 t \tau\rangle' = |{}^3T_1 t \tau\rangle + \frac{\langle {}^3T_1 t \tau | H_{so} | {}^3T_2 t \tau \rangle}{\Delta E}$$

where  $t \tau$  is the coupled function, and the prime refers to the new CI function.

Using the method of Griffith<sup>10</sup> and experimental data the mixing may be calculated by evaluating off-diagonal matrix elements of the form

$$\langle S h J t \tau | H_{so} | S' h' J' t \tau \rangle = \langle S h | \sum_{k=1}^n S \cdot u(k) | S' h' \rangle_{\Omega J J'} \begin{pmatrix} S S' T_1 \\ h' h t \end{pmatrix}$$

In the  $\Omega$  coefficient both  $S$  and  $S' = 1$  and thus

$$\Omega \begin{pmatrix} S S' T_1 \\ h' h t \end{pmatrix} = (-1)^{S'+h+t+1} W \begin{pmatrix} S S' T_1 \\ h' h t \end{pmatrix}$$

In the case we consider, the reduced matrix element can be simplified to the form

$$\langle t_{2g}^5({}^2T_2) e_g^3({}^2E) {}^3T_1 | \sum_k S \cdot u(k) | t_{2g}^5({}^2T_2) e_g^3({}^2E) {}^3T_2 \rangle$$

and is a constant factor in the spin-orbit matrix. It can readily be calculated using the methods given by Griffith<sup>10</sup> and tables of  $W$  and  $\bar{W}$  coefficients since this equals

$$\frac{9\sqrt{3}}{2} \xi \bar{V} \begin{pmatrix} 1/2 & 1/2 & 1 \\ 1 & 1 & 1/2 \end{pmatrix}$$

therefore

$$\langle {}^3T_1 t \tau | H_{so} | {}^3T_2 t \tau \rangle = \Omega \begin{pmatrix} S S' T_1 \\ h' h t \end{pmatrix} \left( \frac{-3\sqrt{3}}{2} \right)$$

Thus the excited-state spin-orbit coupled  $|{}^3T_1 T_1 \tau\rangle'$  function, for example, can now be written as follows

(9) J. S. Griffith, "The Theory of the Transition Metal Ions," Cambridge University Press, London, 1964.

(10) J. S. Griffith, "The Irreducible Tensor Method for Molecular Symmetry Groups," Prentice-Hall, Englewood Cliffs, N. J., 1962.

(11) C. J. Ballhausen and A. D. Liehr, *Mol. Phys.*, **2**, 123 (1959).

(12) T. M. Dunn, *Trans. Faraday Soc.*, 1441 (1961).

(13) W. L. Roth, *Phys. Rev.*, **110**, 1333 (1958).

(14) J. S. Smart, "Molecular Field Theories of Magnetism," W. B. Saunders Co., Philadelphia, Pa., 1966.

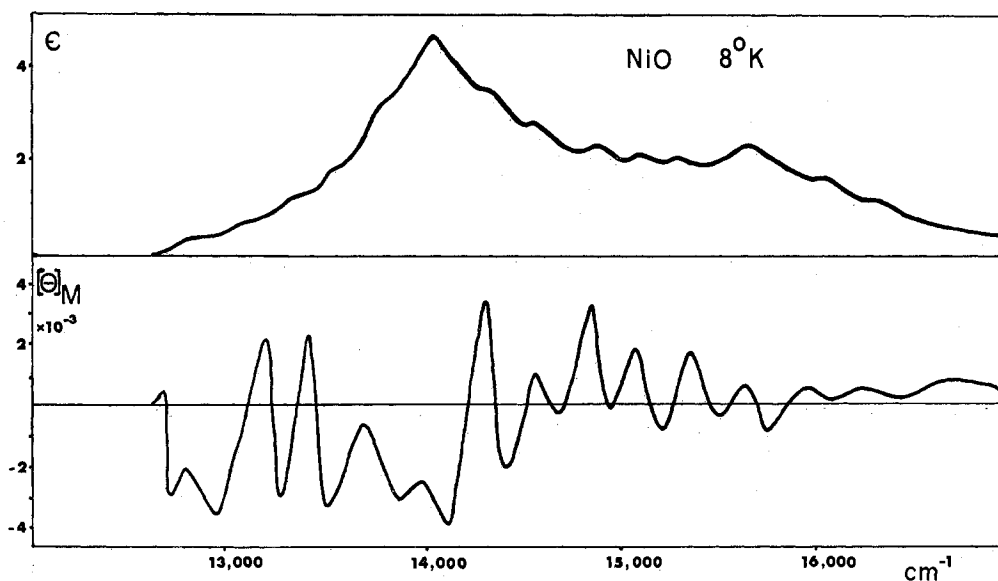


Figure 3.—Absorption and MCD spectra of the "red" band of NiO at 8°K.  $[\theta]_M$  in units of  $\text{deg dl dm}^{-1} \text{mol}^{-1} \text{G}^{-1}$ .

$$\begin{aligned}
 |{}^3T_1T_1\tau\rangle' &= |{}^3T_1T_1\tau\rangle + \left(\frac{-3\sqrt{3}}{2\Delta E}\right)\Omega \begin{pmatrix} 1 & 1 & T_1 \\ T_2 & T & T \end{pmatrix} |{}^3T_2T_1\tau\rangle \\
 &= |{}^3T_1T_1\tau\rangle - \frac{\sqrt{3}}{4\Delta E}\xi |{}^3T_2T_1\tau\rangle
 \end{aligned}$$

*i.e.*, the excited state  $|T_1\tau\rangle'$  function now contains a small admixture of  $|{}^3T_2T_1\tau\rangle$  state which permits electronic transitions by symmetry to the excited  $|T_1\tau\rangle'$  state. The case is similar for the other states of the system. For the example given we may evaluate the coefficient from the experimental data  $\Delta E = 5500 \text{ cm}^{-1}$ ,  $\xi = 650 \text{ cm}^{-1}$  and  $\sqrt{3}\xi/4\Delta E = 0.05$ . Note that the exchange field would cause increased mixing of symmetry-allowed states with those which are forbidden.

With now a mechanism through which transitions are allowed we are able to calculate selection rules for unpolarized light from the conditions under which

$$\langle {}^3A_{2g}T_{2-1} | m^{T_1} | Sht\tau \rangle = \sum_{M\theta} \langle {}^3A_2 - 10 | m^{T_1} | ShM\theta \rangle \langle ShM\theta | Sht\tau \rangle$$

is nonzero. Note that we have obtained this identity from the coupling coefficients in Griffith.<sup>9</sup> As the operator is spin independent

$$= \sum_{\theta} \langle A_2 0 | m^{T_1} | h \rangle \langle h\theta | 1ht\tau \rangle \delta_{S=1} \delta_{M=-1}$$

For this to be nonzero  $h = T_2$ ,  $S = 1$ ,  $M = -1$ . We can then show, using the coupling coefficients, that transitions to E,  $T_{10}T_{1+1}T_{20}$ ,  $T_{2-1}$  of  ${}^3T_1$  are allowed and those to  $A_{10}$ ,  $T_{1-1}$ , and  $T_{2+1}$  are forbidden. We thus expect to see six allowed absorption bands in the region of the  ${}^3T_1$  transition, compared to five if only spin-orbit coupling is important and two if only the crystal field is.

The MCD might be expected to be rather unusual for octahedral  $\text{Ni}^{2+}$  since the exchange field has removed all single ion degeneracies. We should not expect, therefore, to find the dominant  $C$  terms ob-

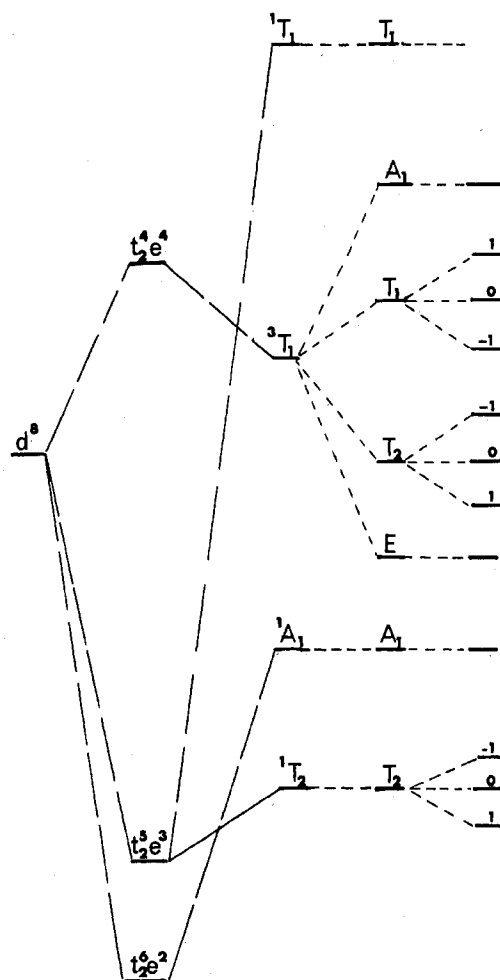


Figure 4.—Energy levels of the "blue" band region of NiO.

served by Mason, *et al.*,<sup>15</sup> in  $\text{Ni}(\text{H}_2\text{O})_6(\text{BrO}_3)_2$ .<sup>16</sup> However, we are left with the sublattice degeneracy since

(15) M. J. Harding, S. F. Mason, D. J. Robbins, and A. J. Thompson, *J. Chem. Soc. A*, 3047 (1971).

(16) Temperature dependent  $C$  terms are also found in the MCD spectra of  $\text{MgO:Ni}^{2+}$ . B. D. Bird, G. A. Osborn, and P. J. Stephens, *Phys. Rev. B*, **5**, 1800 (1972).

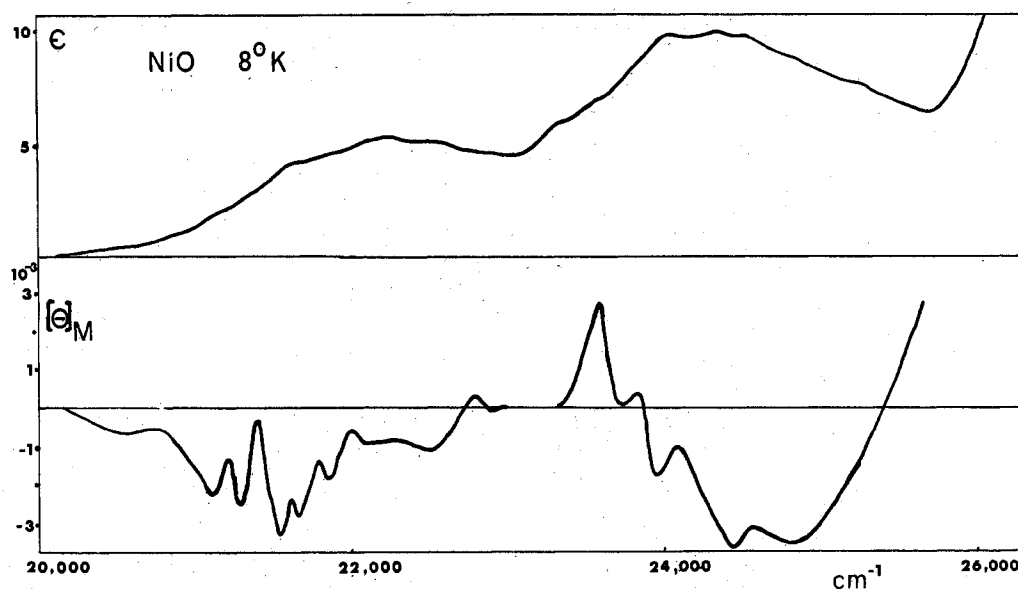


Figure 5.—Absorption and MCD of the "blue" band region of NiO at 7°K. Units as for Figure 3.

the ground state  $T_{2-1}$  on sublattice A is "matched" by  $T_{2+1}$  on sublattice B of identical energy and similarly with the excited states. This is analogous to the splitting of states in an electric field or quantization in a diatomic molecule, and we thus have a twofold degeneracy of all states—the sublattice degeneracy. In the MCD experiment, therefore, we expect to see A terms arising from the Zeeman splitting of the sublattice degeneracy as shown in Figure 2. The signs of these A terms have been calculated for the six transitions in a similar fashion to that described for the unpolarized absorption, through now the operators used are  $m_+$ ,  $m_-$  for left and right circularly polarized light, respectively. A summary of these calculations is given in Table I.

TABLE I  
SUMMARY OF MCD CALCULATIONS "RED" BAND REGION

$T_{10}$	positive	$T_{2-1}$	zero
$T_{1+1}$	zero	$E(^3T_1)$	positive
$T_{20}$	positive	$E(^1E)$	positive

The experimental absorption at  $\sim 8^\circ\text{K}$  (Figure 3) in the red region consists of a number of prominent peaks which have smaller shoulders associated with them. Our analysis of this structure (see Table II) leads us

TABLE II  
OBSERVED ABSORPTION BANDS AND BAND ASSIGNMENTS,  
 $T_{1-1} \rightarrow$

$T_{10}$	$T_{1+1}$	E	$T_{20}$	$T_{2-1}$	E	
12,849	13,050	14,029	14,870	15,074	15,656	
13,094	13,312	14,316	15,168	15,313	15,898	
13,350	13,550	14,558	15,380		16,155	
13,624	13,831				16,394	
$T_{20}$	$T_{2-1}$	E	$T_{20}$	$T_{2-1}$	$T_{10}$	$T_{1+1}$
20,920	21,110	23,360	23,870	24,060	24,330	24,510
21,170	21,370	23,580			24,870	24,752
21,420	21,620					
21,680	21,860					
21,940	22,140					
22,670	22,660					

to identify six peaks in the absorption spectrum at 12,849, 13,050, 14,029, 14,870, 15,074, and 15,656

$\text{cm}^{-1}$ , and with each of these are associated several quanta of a lattice vibration of  $245 \text{ cm}^{-1}$ . These are identified in Table II. This agrees reasonably with one of the phonon frequencies of NiO having  $t_{1u}$  symmetry.<sup>8b</sup> On the basis of the calculations above, these six bands are assigned as  $T_{10}$ ,  $T_{1+1}$ , E,  $T_{20}$ ,  $T_{2-1}$ , and E, respectively. The agreement with calculation is quite good and suggests an excited-state exchange field of  $\sim 200 \text{ cm}^{-1}$ . This is somewhat larger than the ground state value and may indicate some change in the excited-state molecular field, though in view of the approximations made in the calculations this conclusion could only be very tentative. From Table II we note the near identity of the  $T_{10}$ - $T_{1+1}$  and  $T_{20}$ - $T_{2-1}$  energy splittings which is strong evidence for the validity of this approach.

The MCD spectrum shows the A term structure expected from the foregoing discussion and under the absorption region at low temperature appears a succession of A terms. We have picked out MCD's associated with the four lines which can show MCD and their phonon side bands, and although there is a certain arbitrariness in deciding the signs in regions of overlap, we find them to be in agreement with calculation.

The other main region of the spectrum ( $20$ - $26,000 \text{ cm}^{-1}$ ) does not show the detailed fine structure of the "red" band, though structure does appear at low temperature. By analogy to the  $\text{MgO:Ni}^{2+}$  spectrum<sup>8</sup> and the crystal field calculations<sup>11</sup> the two bands at  $\sim 22,300$  and  $24,300 \text{ cm}^{-1}$  are predominantly  $^1A_{1g} + ^1T_{2g}$  and  $^3T_{2g}$ , respectively, though we note an increased degree of intensity sharing between singlet and triplet in the case of NiO. This would be expected to arise from the exchange field. Figure 5 shows the new states of  $^1A_1$ ,  $^1T_2$ ,  $^3T_2$  after the effects of spin-orbit coupling and exchange field have been taken into account and the selection rules, as before, are that  $T_{2+1}$ ,  $A_1$ , and  $T_{1-1}$  are forbidden excited states for unpolarized absorption and that  $T_{2-1}$ ,  $T_{1+1}$  should show no MCD. From analysis of the data (Table I), we make identifications as follows:  $T_{20}$ ,  $T_{2-1}$  (from  $^1T_2$ ), E,  $T_{20}$ ,  $T_{2-1}$ ,  $T_{10}$ ,  $T_{1+1}$ , (from  $^3T_1$ ) at 20,920, 21,110, 23,360, 23,870, 24,060, 24,330, and 24,510  $\text{cm}^{-1}$ .

The exchange field splittings are all around 190  $\text{cm}^{-1}$  with these assignments.

The MCD in this region is not very well defined, except for the region around 21,000  $\text{cm}^{-1}$ , and it is difficult to make clear assignments of features to absorption peaks due to the overlap of phonons in the first band of this region, but the MCD is generally consistent with this assignment. Above 26,000  $\text{cm}^{-1}$  an intense absorption sets in which could not be penetrated optically. This presumably represents a charge-transfer transition and gives an indication of the energy barrier ( $\sim 3.5$  eV) in the conduction process as electrons are transferred from nickel ion to nickel ion throughout the lattice.

### Conclusion

Previous interpretations of the spectrum of NiO have assumed the model of a  $d^8$  ion perturbed only by the crystal field. We find this approximation is not able to explain the details of the absorption spectrum

at liquid helium temperatures and is completely inadequate for describing the MCD. We have found that it is essential to include explicitly the exchange field and have obtained a good fit to experiment using a molecular field model with  $H_E$  190  $\text{cm}^{-1}$ , somewhat larger than the ground-state exchange field. We conclude that in NiO and in other antiferromagnets where  $H_E \sim kT$ , the effect should be included. The regions of the spin-forbidden regions are not sufficiently sharp at low temperatures for us to identify magnon side bands or magnon assistance in the spectra.

**Acknowledgments.**—We wish to thank Dr. Smith of the Clarendon Laboratory for the loan of the NiO sample and the Science Research Council for financial support and for studentships to P. B., R. G., and M. D. R. We also thank Dr. D. W. Copsey for helpful discussion on the theoretical aspects of electronic states of antiferromagnets.

CONTRIBUTION FROM THE CENTER OF MATERIALS RESEARCH AND THE DEPARTMENT OF CHEMISTRY, UNIVERSITY OF MARYLAND, COLLEGE PARK, MARYLAND 20742

## X-Ray Photoelectron Spectroscopy of Tin. I. Hexahalostannates

BY WILLIAM E. SWARTZ, JR.,\*<sup>1a</sup> PLATO H. WATTS, JR.,<sup>1a,b</sup> ELLIS R. LIPPINCOTT,<sup>1a,b</sup> JUDITH C. WATTS,<sup>1b</sup> AND JAMES E. HUHEEY<sup>1b</sup>

Received February 9, 1972

X-Ray photoelectron spectroscopy (ESCA) has been used to measure the tin ( $3d_{5/2}$ ) electron binding energies for octahedral tin complexes of formula  $[(\text{CH}_2\text{CH}_2)_4\text{N}]_2[\text{SnX}_{6-n}\text{Y}_n]$ . The binding energies are found to correlate linearly with average ligand electronegativities, Mössbauer isomer shifts, and estimated atomic charges on the tin atom. The results are discussed in terms of these molecular parameters.

### Introduction

Although there is still some uncertainty concerning the exact relation between core-electron binding energies measured *via* X-ray photoelectron spectroscopy (ESCA) and atomic charges,<sup>2-7</sup> this technique promises to be a useful tool in determining the electronic environment of atoms in molecules. ESCA binding energies have been shown to correlate with ligand electronegativities for a rather large number of compounds.<sup>2,5,8</sup> In addition, Gelius and coworkers<sup>9</sup> have calculated group electronegativities for a large number of organic functional groups using ESCA data. Barber and coworkers<sup>10</sup> have reported a linear relationship between the Mössbauer isomer shifts of <sup>119</sup>Sn and the tin (4d) binding energies for some tin complexes in

which the tin atom had constant stereochemistry and oxidation state. The authors point out that since Mössbauer data have been shown to correlate with ligand electronegativity,<sup>11-14</sup> their data further verify the correlation between ESCA binding energies and ligand electronegativities. Several workers<sup>5,15-20</sup> have attempted to correlate measured electron binding energies with atomic charges obtained from calculative techniques of varying degrees of sophistication. In this article we wish to report an ESCA study of octahedral tin in hexahalostannates of formula  $[(\text{CH}_2\text{CH}_2)_4\text{N}]_2[\text{SnX}_{6-n}\text{Y}_n]$ , in which the tin ( $3d_{5/2}$ ) electron binding energies are found to correlate with the average electronegativities of the halide ligands, the Mössbauer isomer shifts reported for the compounds, and

- (1) (a) Center of Materials Research. (b) Department of Chemistry.
- (2) J. M. Hollander and W. L. Jolly, *Accounts Chem. Res.*, **3**, 193 (1970).
- (3) M. Barber and D. T. Clark, *Chem. Commun.*, **22**, 23, 24 (1970).
- (4) A. van der Avoird, *ibid.*, 727 (1970).
- (5) K. Siegbahn, C. Nordling, A. Fahlman, R. Nordberg, K. Hamrin, J. Hedman, G. Johansson, T. Bergmark, S. E. Karlson, I. Lindgren, and B. Lindberg, "ESCA; Atomic, Molecular, and Solid State Structure Studied by Means of Electron Spectroscopy," Almqvist and Wiksells, Uppsala, 1967.
- (6) D. T. Clark, D. B. Adams, and D. Briggs, *Chem. Commun.*, 602 (1971).
- (7) W. L. Jolly, *J. Amer. Chem. Soc.*, **92**, 3260 (1970).
- (8) T. D. Thomas, *ibid.*, **92**, 4184 (1970).
- (9) U. Gelius, P. F. Heden, J. Hedman, B. J. Lindberg, R. Manne, R. Nordberg, C. Nordling, and K. Siegbahn, *Phys. Scr.*, **2**, 70 (1970).
- (10) M. Barber, P. Swift, D. Cunningham, and M. J. Frazer, *Chem. Commun.*, 1338 (1970).

- (11) K. M. Ali, D. Cunningham, J. D. Donaldson, M. J. Frazer, and B. J. Senior, *J. Chem. Soc. A*, 2836 (1969).
- (12) R. H. Herber and H. S. Cheng, *Inorg. Chem.*, **8**, 2145 (1969).
- (13) C. A. Clausen and M. L. Good, *ibid.*, **9**, 817 (1970).
- (14) M. O'Rourke and C. Curran, *J. Amer. Chem. Soc.*, **92**, 1501 (1970).
- (15) J. M. Hollander, D. M. Hendrickson, and W. L. Jolly, *J. Chem. Phys.*, **49**, 3515 (1968).
- (16) M. Pelavin, D. N. Hendrickson, J. M. Hollander, and W. L. Jolly, *J. Phys. Chem.*, **74**, 1116 (1970).
- (17) D. N. Hendrickson, J. M. Hollander, and W. L. Jolly, *Inorg. Chem.*, **8**, 2642 (1969); **9**, 612 (1970).
- (18) H. Basch and L. C. Snyder, *Chem. Phys. Lett.*, **3**, 333 (1969).
- (19) D. W. Davis, J. M. Hollander, D. A. Shirley, and T. D. Thomas, *J. Chem. Phys.*, **52**, 3295 (1970).
- (20) P. Finn, R. K. Pearson, J. M. Hollander, and W. L. Jolly, *Inorg. Chem.*, **10**, 378 (1971).